

## Design and Synthesis of quinazoline derivatives: Biological evaluation for their Anticancer and VEGFR inhibitory activities.

Wegdan M. Metwally<sup>a\*</sup>, Gehan Hegazy<sup>b</sup>, Sameh Eid<sup>d</sup>, Rabah A.T. Serya<sup>d</sup>, Dalal A. Abou El Ella<sup>d</sup>.

<sup>a</sup> Department of Pharmaceutical Chemistry, Faculty of Pharmacy, Modern Science and Arts University, 6th of October City, Cairo, Egypt

<sup>b</sup> Department of Pharmaceutical Chemistry, Faculty of Pharmacy, Cairo University, Kaser-El-Eni, Cairo, Egypt.

<sup>c</sup> Department of Pharmaceutical Sciences, University of Basel, Biozentrum, Klingelbergstrasse 50, 4056 Basel, Switzerland.

<sup>d</sup> Department of Pharmaceutical Chemistry, Faculty of Pharmacy, Ain Shams University, Abbasia, Cairo, Egypt.  
[wegdan\\_metwally@hotmail.com](mailto:wegdan_metwally@hotmail.com)

**Abstract:** In this thesis a series of novel 4-substituted quinazoline derivatives was rationally designed, synthesized and biologically evaluated for their anticancer activity. The sixteen synthesized compounds **IVa-f**, **Va-d**, **VIa-d** and **VIIa, b** were evaluated for their antitumor activity against MCF7 and HEPG2 cell lines at National Cancer Institute (NCI, Egypt). Eight of these compounds **IVc**, **IVf**, **Vc**, **VIa-d**, **VIIb** were selected due to their promising activity against the cell lines to be tested *in vitro* against VEGFR2 inhibition in KINEXUS cooperation, Canada. Compound **VIa** show marked inhibitory activity against VEGFR2 (52%). The obtained results were clarified using molecular modeling study using grid-based ligand docking with energetics glide program. The design depends on exploration of the previous revealed SAR studies, identification of the key interactions with the binding site and bioisosteric modifications of the reference compound **6**.

[Wegdan M. Metwally, Gehan Hegazy, Sameh Eid, Rabah A.T. Serya, Dalal A. Abou El Ella. **Design and Synthesis of quinazoline derivatives: Biological evaluation for their Anticancer and VEGFR inhibitory activities.** *Life Sci J* 2016;13(2):57-68]. ISSN: 1097-8135 (Print) / ISSN: 2372-613X (Online). <http://www.lifesciencesite.com>. 10. doi:10.7537/marslsj13021610.

**Key words:** Anticancer; quinazoline derivatives, kinase inhibitors

### 1. Introduction

The control of disseminated tumor growth by systemically active chemotherapeutic agents remains a major challenge for cancer chemotherapy despite decades of focused efforts. Although there are some notable successes with certain forms of cancer, drug therapy has only limited impact against the three major killers: Carcinoma of the lung, breast, and colorectal system [1].

Vascular endothelial growth factor (VEGF) is a potent mitogen that is highly specific for vascular endothelial cells [2, 3], and is a highly potent angiogenic agent that increases vessel permeability and enhances endothelial cell growth, proliferation, migration, and differentiation [4]. VEGF isoforms and their cognate tyrosine kinase receptors (VEGFRs) have been especially attractive targets for the inhibition of angiogenesis [5]. One important advantage of angiogenesis inhibitors is that, they do not target the cancer cells directly; there is less chance that the cancer cells will develop resistance to the drug [6].

VEGFR-1 is expressed on hematopoietic stem cells, macrophages and monocytes as well as on the vascular endothelium. VEGFR-2 is expressed on both vascular and lymphatic endothelium, whereas expression of VEGFR-3 is generally restricted to

lymphatic endothelium. The vascular endothelium is composed of a single layer of endothelial cells with tight inter-endothelial junctions, surrounded by basement membrane and stabilized by specialized smooth muscle cells, called pericytes. In contrast, the lymphatic endothelium lacks inter-endothelial junctions, basement membrane and supporting pericytes allowing for the permeability of lymphatic vessels [7].

In 1971, Folkman first proposed the theory that inhibition of angiogenesis may result in the arrest of tumor growth [7]. This vision has now become a reality, with the arrival of a number of anti-angiogenic drugs in the clinic [8, 9]. Anti-angiogenic compounds are postulated to not only reduce tumor vascularization, but also create a more stable, or normalized, vasculature within the tumor, enabling efficient delivery of anti-tumor drugs [10].

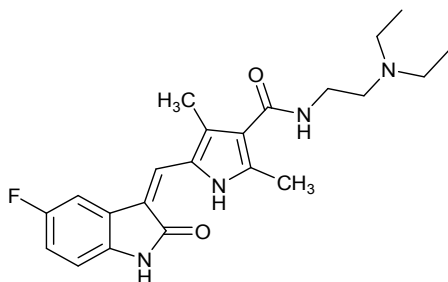
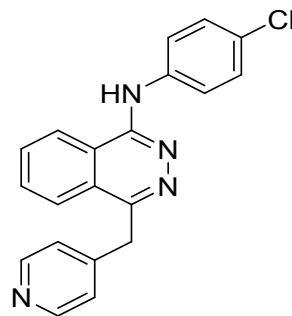
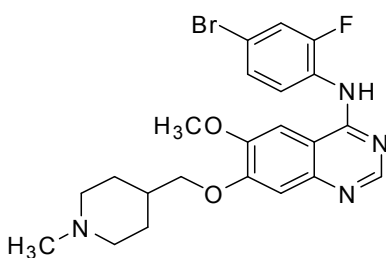
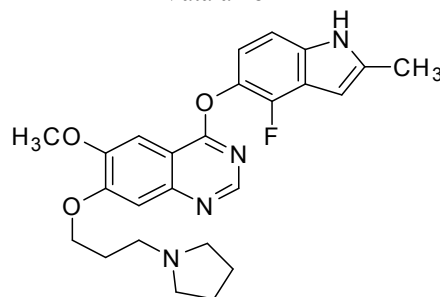
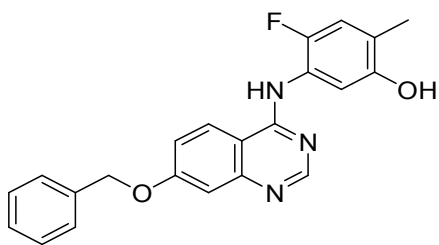
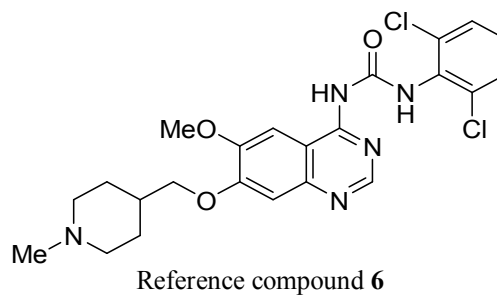
The biological effects of VEGF are mediated by mainly two receptor tyrosine kinases (RTKs), VEGFR-1 [11], kinase and VEGFR-2 kinase [12]. It has been demonstrated that the inhibition of VEGF signaling not only blocks angiogenesis in tumors but can also change or destroy tumor vessels [13]. Therefore, VEGFR-2 is an attractive target for biological cancer therapies.

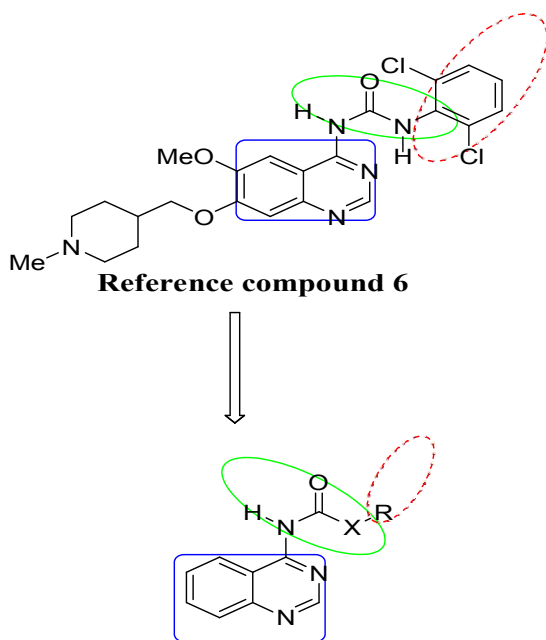
Sunitinib **1** is an indole derivative with dual-target RTK inhibitor to VEGFR-2 and platelet-derived growth factor receptor PDGFR- $\beta$ , which exhibits anti-tumor activity [14]. Vatalanib **2** is an orally active anilinoquinazoline inhibitor of VEGFR 1 and 2, as well as PDGFR and c-Kit at higher concentrations [15].

Quinazolines were initially developed as EGFR-TK inhibitors. Vandetanib **3** [16], is one of the quinazoline family being evaluated in several phase II clinical trials. Vandetanib **3** is a heteroaromatic substituted anilinoquinazoline, which has been shown to inhibit VEGF signaling, tumor-induced neovascularisation and growth of xenograft tumor models *in vivo* [7]. It occupies the adenosine triphosphate ATP adenine binding site, where it forms a single hydrogen bond involving its N-1 nitrogen and the Cys-912 residue of the protein. Other promising quinazoline derivatives that act on VEGFR is cediranib AZD-2171 **4** [17, 18], which demonstrated

>800- to 5000-fold *in vitro* selectivity for VEGFR-2 inhibition, compared with a range of tyrosine and serine-threonine kinases. It is undergoing a number of clinical trials (Phase I, II and III) to evaluate its role in a range of solid tumors [18]. It is a potent ATP-competitive, sub-nanomolar inhibitor of VEGFR-2. It has been shown to inhibit VEGF-R induced proliferation and VEGFR-2 phosphorylation in human umbilical endothelial cells HUVEC and also to inhibit angiogenesis *in vivo* [19].

An example of recent US FDA approved of small molecule inhibitors of VEGFR protein tyrosine kinases is ZM323881 **5** [20], which is a potent and selective inhibitor of VEGFR-2 tyrosine kinase *in vitro* ( $IC_{50} < 2$  nM), compared with other receptor tyrosine kinases, including VEGFR-1 ( $IC_{50} > 50$   $\mu$ M). Another patent quinazolinyureas derivative **6** as VEGF receptor antagonists is under different phases of clinical trials [21].

Sunitinib(SU-112 48) **1**Vatalanib **2**Vandetanib (ZD-6474) **3**Cediranib, AZD-2171 **4**ZM-323881 **5**Reference compound **6**



R: different aryl or heterocyclic ring.  
X: CH<sub>2</sub>, CH-CH<sub>3</sub>, NH.

#### Target compounds IVa-f, Va-d, VIa-d and VIIa-b

	Maintaining the quinazoline ring which mimic the binding mode of ATP to the hinge region of the kinase active site.
	Keeping the urea moiety, replacement with amide or thioamide which may show the same binding interactions with Glu883
	Different substituent keeping the same hydrophobic binding interactions

**Figure 1: Similarities between reference compound 6 and target compounds IVa-f, VIa-d and VIIa-b**

Consequently, the objective of this research is to design new quinazoline derivatives hoping to act as type 2 inhibitors targeting VEGFR-2 by keeping the essential interacting features as reported. Type-2 inhibitors provide a superior kinetic advantage over type-1 inhibitors as they avoid competition with ATP on the active site and stabilize the kinase in the DFG-out conformation which is the inactive conformation [22]. By exploring the SAR, it has been found that these inhibitors that contains the quinazoline ring binds to the hinge region of the kinase [23], but the most important here is the substitution at position 5 or 4 of the the quinazoline, which play an important role in selectivity. The substitution at 4 position of the quinazoline ring always contains aryl or heterocyclic moiety and this is the reason behind the stabilization of the DFG out conformation of the DFG motif. Where a hydrogen bond acceptor adjacent to a

hydrogen bond donor between the quinazoline ring and the additional aryl or heterocyclic moiety is commonly used, which bind to the DFG motif of the kinase and the far ring system extends to bind to a binding pocket found only in the inactive form of the kinase. According to the previous finding of the key interactions within the VEGFR2, a new series of quinazoline molecules was designed as VEGFR-2 inhibitors based on the following modification strategies hoping to have the same binding interactions obtained from the previous data where, two hydrogen bond with the side chain of a conserved glutamic acid in the C-helix (Glu 883) and one hydrogen bond with the backbone amide of aspartic acid in the DFG motif (Asp 1044) may be formed. Additionally, the hydrophobic moiety that is located immediately after the hydrogen bond donor-acceptor pair may forms hydrophobic interactions with the

allosteric site. Main scaffold (quinazoline nucleus) occupying the ATP binding site was kept. The linker was designed to be urea, thiourea or amide moiety. The aryl moiety, essential for allosteric site binding was conserved. Out of this study, a new series of quinazoline molecules were designed in order to be prepared and evaluated as VEGFR-2 inhibitors based on the following criteria illustrated in figure 1.

## 2. Results and discussion

### 2.1 Chemistry

Synthetic approaches for the target compounds based upon the acetylation of 4-amino quinazoline with chloroacetyl chloride or 2-bromopropionyl chloride to give compound **II** and **III** respectively. Coupling of these intermediates with amine derivative to give **IVa-f** and **Va-d** as shown in scheme 1. On the other hand the targeted urea derivatives **VIa-d** were prepared in very good yield by refluxing the 4-aminoquinazoline with the appropriate isocyanate or isothiocyanate derivatives in proper solvent as shown in scheme 2. The addition of the appropriate amine to compound **VIc** yields compounds **VIIa-b** as shown in scheme 2.

IR, <sup>1</sup>HNMR spectra and elemental analyses were used for determination and identification of the newly assigned structures.

### 2.2 Biological activity

#### 2.2.1 *In vitro* anticancer activity Table 1:

The compounds were submitted to the National Cancer Institute, Egypt to test their *in vitro* anticancer activity by screening against MCF7 and HEPG2 cell lines. Potential cytotoxicity of the selected compounds were tested using the method of Skehan *et al.* [24]. The results which obtained are shown in **Table 1**.

#### 2.2.2 Enzyme inhibitory activity assay against VEGFR2 Table 2:

Eight of the new compounds were chosen due to their promising anticancer activity to perform enzyme inhibitory activity against VEGFR2. Enzyme inhibition assay was performed in KINEXUS Corporation Vancouver, BC, Canada [25].

The kinase inhibitory activity of the selected compounds were assayed by ELISA. The assay was against VEGFR. The inhibitory activity was given as percentage inhibition at concentration 10 $\mu$ m. The profiling data for various compounds against VEGFR2 show weak inhibitory activity except compound **VIa** which show 52% inhibition. The results are shown in **Table 2**.

### 2.3 Molecular modeling

In order to explore the binding mode inside the ATP binding site of the targeted kinases a comprehensive docking experiment was done using Glide (Grid-based Ligand Docking with Energetics) which is a widely used software package for docking

small-molecule ligands to macromolecular protein targets [26-33]. Several studies have shown Glide's superiority in predicting and properly ranking binding configurations of ligands to their protein targets [34-36]. Glide employs a rigid-receptor approximation where ligands are docked into a single static representation of the binding site residues.

**Table 1: The activity of the tested compounds on hepatic and breast cell lines:**

Compound	IC <sub>50</sub> (ug/ml)	
	HEPG2	MCF7
Doxorubicin	3.68	4.28
IVa	15.80	15.90
IVb	20.90	18.20
IVc	17.30	5.05
IVd	18.70	15.80
IVe	17.90	7.40
IVf	11.20	11.20
Va	13.40	14.90
Vb	23.00	9.00
Vc	3.04	3.90
Vd	21.80	13.30
VIa	7.28	4.43
VIb	11.00	4.80
VIc	10.70	14.10
VId	3.68	3.75
VIIa	16.50	18.50
VIIb	16.00	11.30

**Table 2: Percentage inhibition of enzymatic activity for the targeted compounds of VEGFR2 Kinase.**

Compound	% inhibition of VEGFR2 kinase (10 $\mu$ m)
IVc	14
IVf	19
Vc	9
VIa	52
VIb	1
VIc	12
VId	2
VIIb	11

The proposed docking algorithm was validated by self-docking in the VEGFR crystal structure (PDB code 2OH4) [37] by removing the co-crystallized benzimidazole-urea inhibitor **6** from the complex then

docking it back into the binding site. The RMSD value is 0.25 Å which shows that Glide can yield reliable

docking poses for the modeled compound as shown in figure 2:

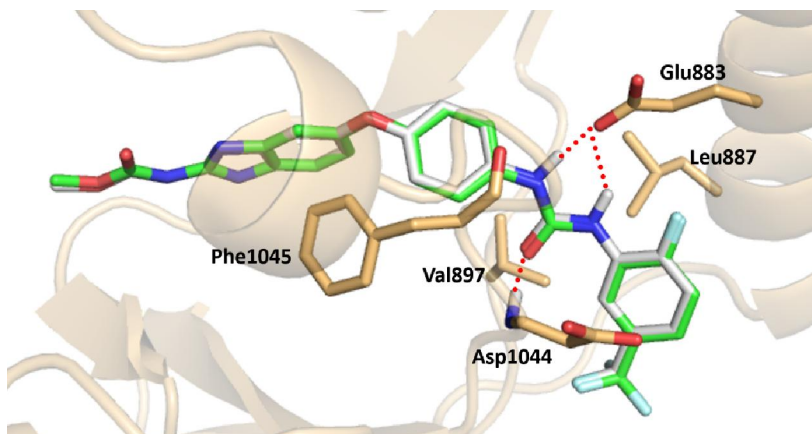


**Figure 2: Redocking of benzimidazole-urea inhibitor in complex with VEGFR2 (PDB code 2OH4); white carbons: crystal structure pose, green carbons: top-ranked docking pose. Protein atoms and cartoons are colored orange. Hydrogen bonds are represented by red dotted lines.**

### Glide docking

Top-ranked poses obtained from Glide XP docking for compound **VIa** to VEGFR2 (Figure 2) bear a significant degree of similarity to the inhibitor present in solved crystal structure. For instance, in both poses compound **VIa** establishes the same hydrogen network between the urea moiety and the side chain carboxylate of Glu883 and backbone NH of Asp1044. The two top-scored poses are related by a flipping of the urea moiety around the central carbonyl group. In the first pose, the hydrophobic

pocket between Phe1045 and Val897 was filled by the chlorophenyl group of compound **VIa**, while the quinazoline moiety packed against the side chains of Asp1044 and Leu887. In the second pose, the two roles are interchanged as shown in figure 3. Therefore, docking results indicate that compound **VIa** can be accommodated in the binding site of VEGFR2 and establish a network of interactions comparable to the reported inhibitor, which could explain the potent inhibition observed in the enzymatic assay.

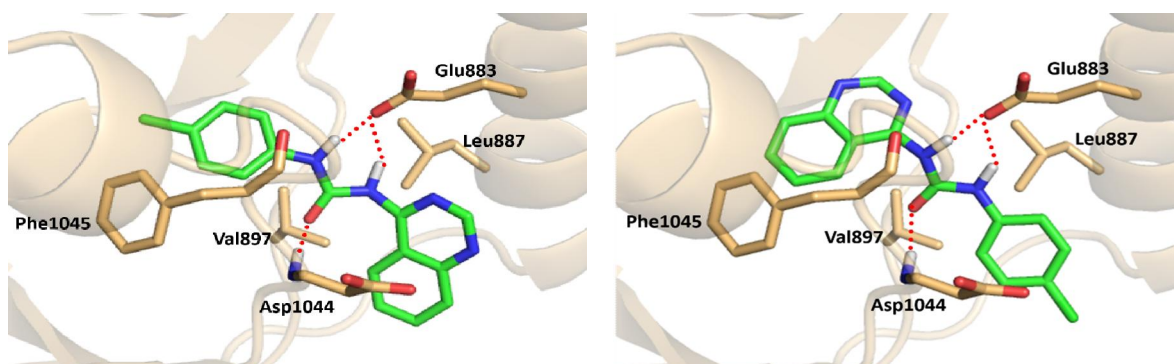


**Figure 3: Top-ranked docking poses of compound **VIa** to VEGFR2 maintain the key interactions exhibited by the co-crystallized inhibitor in PDB 2OH4. Protein atoms and cartoons are colored orange. Hydrogen bonds are represented by red dotted lines.**

### 3. Conclusion:

A novel series of quinazoline derivatives have been designed and synthesized, where their anticancer activity was tested against MCF7 and HEPG2 cell lines in NCI, Egypt. Anticancer activity revealed that compounds **Vc**, **VIa**, **VIc** **VI d** have significant anticancer activity on hepatic cell line with  $IC_{50}$  3.04,

7.28, 10.70 and 3.68  $\mu\text{g/ml}$ , respectively. Also compounds **IVc**, **IVe**, **IVf**, **Vc**, **VIa**, **VIb**, and **VI d**, **VIIb** showed moderate to high activity against breast cell line with  $IC_{50}$  5.05, 7.40, 11.20, 3.90, 4.43, 4.80 and 3.75 and 11.30  $\mu\text{g/ml}$  respectively.

The compounds **IVc**, **IVf**, **Vc**, **VIa-d**, **VIIb** were selected due to their promising anticancer activity to



test their *in vitro* enzyme inhibition activity where unfortunately, they show weak inhibition enzyme activity except compound **VIa** which has the highest percentage of VEGFR-2 inhibition (52%) at 10  $\mu$ m. The good inhibition activity of this compound was explained using docking study which revealed that the presence of urea moiety attached to the *p*-chlorophenyl in position 4 maintains the same hydrogen network between the urea moiety and the side chain carboxylate of Glu883 and backbone NH of Asp1044 as the benzimidazole inhibitor and the reference compound **6**.

It was clear that the presence of the phenyl piperazine ring in certain compounds such as **IVc** and **Vc** play an important role in their activity against breast MCF7 and hepatic HEPG2 cell lines. The substitution in the phenyl piperazine ring in compounds **IVe** and **IVf** decreases their activity. Also, the thiourea moiety in compound **VIId**, play an important role in the activity but, the exact inhibitory mechanism of these compounds could not be fully described but still a material for future investigation.

## 4. Experimental

### 4.1 Chemistry

Melting points determined in one end open capillary tubes using Stuart Scientific apparatus and were uncorrected. The NMR spectra were recorded on a Perkin-Elmer,  $^1\text{H}$  spectra were run at 500 MHz. EI-MS spectra were recorded on Finnigan Mat SSQ 7000 (70 eV) mass spectrometer at Micro analytical Centre at Cairo University (Varian, Polo, USA). Analytical thin layer chromatography (TLC) was performed on silica gel 60 F254 packed on Aluminium sheets, purchased from Merck (Merck, Darmstadt, Germany). FT-IR spectra were recorded on a Perkin-Elmer spectrophotometer at faculty of science Cairo University.

#### 4.1.1 General procedure for preparation of 2-substituted-(*N*-quinazolin-4-yl)-acetamide derivatives (**IVa-f**) and 2-substituted-(*N*-quinazolin-4-yl)-propionamide derivative (**Va-d**):

A suspension of compound **II** or **III** (10.00 mmol) was heated under reflux in absolute ethanol (15 mL) for 8-12 hrs with the corresponding amine (2.00 mmol), in presence of catalytic amount of TEA (20.00 mmol). The excess ethanol was evaporated under vacuum; the residue was treated with 5% sodium bicarbonate solution to remove acid impurities, filtered, washed with water. The crude product was dried and crystallized from ethanol to afford the titled compound **IVa-f** and **Va-d** respectively.

##### 4.1.1.1 4-Chloro-2-[(quinazolin-4-yl)-carbamoylmethyl]-aminol-benzoic acid (**IVa**):

Yield 75%; m.p 220-221°C. Analysis for  $\text{C}_{17}\text{H}_{13}\text{ClN}_4\text{O}_3$  (m.w 356); calcd: C, 57.23; H, 3.67, N,

15.70, Found: C, 56.97, H, 3.80, N, 15.80. **IR (KBr,  $\text{cm}^{-1}$ ):** 3482-3200 (OH acid), 3365-3354 (2NH), 1687 (C=O amide), 1753 (C=O acid)  $^1\text{HNMR}$  (DMSO- $d_6$ , ppm) 4.10 (s, 2H,  $\text{CH}_2$ ), 6.40-6.68 (m, 3H, aromatic protons), 7.70-8.37 (m, 5H, quinazoline), 8.70 (s, 2H, 2NH) ( $\text{D}_2\text{O}$  exchangeable); 9.90 (s, 1H, OH) ( $\text{D}_2\text{O}$  exchangeable); **MS** (m/z): 356.40, ( $\text{M}^+$ , 3.18%).

##### 4.1.1.2 2-Indol-1-yl-*N*-quinazolin-4-yl-acetamide (**IVb**):

Yield 74.7%; m.p 120-122°C. Analysis for  $\text{C}_{18}\text{H}_{14}\text{N}_4\text{O}$  (m.w 302); calcd: C, 71.51; H, 4.67, N, 18.53, Found: C, 71.53, H, 4.57, N, 18.53. **IR (KBr,  $\text{cm}^{-1}$ ):** 3431 (NH), 1689 (C=O),  $^1\text{HNMR}$  (DMSO- $d_6$ , ppm): 3.00 (s, 2H,  $\text{CH}_2$ ), 6.40-7.50 (m, 6H, indole), 7.71-8.40 (m, 5H, quinazoline), 8.40 (s, 1H, NH) ( $\text{D}_2\text{O}$  exchangeable); **MS** (m/z) 302.30 ( $\text{M}^+$ , 1.09%).

##### 4.1.1.3 2-(4-Phenyl-piperazin-1-yl)-*N*-quinazolin-4-yl-acetamide (**IVc**):

Yield 73.17%; m.p 205-206°C. Analysis for  $\text{C}_{20}\text{H}_{21}\text{N}_5\text{O}$  (m.w 347); calcd: C, 69.14, H, 6.09, N, 20.16, Found: C, 68.95, H, 6.2, N, 19.88. **IR (KBr,  $\text{cm}^{-1}$ ):** 3424 (NH), 1674 (C=O),  $^1\text{HNMR}$  (DMSO- $d_6$ , ppm): 2.80 (s, 2H,  $\text{CH}_2$ ), 2.95 (t,  $J = 6.2$  Hz, 4H, 2( $\text{CH}_2$ )), 3.18 (t,  $J = 6.0$  Hz, 4H, 2( $\text{CH}_2$ )), 6.60-7.27 (m, 5H, aromatic protons), 6.80-7.90 (m, 5H, quinazoline), 8.50 (s, 1H, NH) ( $\text{D}_2\text{O}$  exchangeable); **MS** (m/z) 347.30 ( $\text{M}^+$ , 9.11%).

##### 4.1.1.4 2-Morpholine-4-yl-*N*-quinazolin-4-yl-acetamide (**IVd**):

Yield 83.33%; m.p 210-212°C. Analysis for  $\text{C}_{14}\text{H}_{16}\text{N}_4\text{O}_2$  (m.w 272); calcd: C, 61.75, H, 5.92, N, 20.58, Found C, 61.12, H 5.82, N 20.92. **IR (KBr,  $\text{cm}^{-1}$ ):** 3419 (NH), 1662 (C=O),  $^1\text{HNMR}$  (DMSO- $d_6$ , ppm): 2.40 (t,  $J = 6.2$  Hz 4H, 2( $\text{CH}_2$ )), 3.32 (s, 2H,  $\text{CH}_2$ ), 3.71 (t,  $J = 6.0$  Hz 4H, 2( $\text{CH}_2$ )), 7.50-8.20 (m, 5H, quinazoline), 8.39 (s, 1H, NH) ( $\text{D}_2\text{O}$  exchangeable); **MS** (m/z) 272.30, ( $\text{M}^+$ , 9.18%).

##### 4.1.1.5 2-[4-(4-Nitro-phenyl)-piperazin-1-yl]-*N*-quinazolin-4-yl-acetamide (**IVe**):

Yield 79.71%; m.p 165-166°C. Analysis for  $\text{C}_{20}\text{H}_{20}\text{N}_6\text{O}_3$  (m.w 392); calcd: C, 61.21, H, 5.14, N, 21.42. Found C, 61.75, H, 5.32, N, 21.50. **IR (KBr,  $\text{cm}^{-1}$ ):** 3388 (NH), 1680 (C=O), 1588, 1392 ( $\text{NO}_2$ ),  $^1\text{HNMR}$  (DMSO- $d_6$ , ppm): 3.33 (s, 2H,  $\text{CH}_2$ ), 3.46 (t,  $J = 6.2$  Hz, 4H, 2( $\text{CH}_2$ )), 3.49 (t,  $J = 6.0$  Hz, 4H, 2( $\text{CH}_2$ )), 7.30-7.41 (m, 4H, aromatic proton), 7.42-8.38 (m, 5H, quinazoline), **MS** (m/z) 392.40, ( $\text{M}^+$ , 0.17%).

##### 4.1.1.6 2-[4-(2-Methoxyphenyl)-piperazin-1-yl]-*N*-quinazolin-4-yl-acetamide (**IVf**):

Yield 67.36%; m.p 165-166°C. Analysis for  $\text{C}_{21}\text{H}_{23}\text{N}_5\text{O}_2$  (m.w 377); calcd: C, 66.83, H, 6.14, N, 18.55, Found C, 66.80, H, 6.10, N, 18.50. **IR (KBr,  $\text{cm}^{-1}$ ):** 3429 (NH), 1681 (C=O),  $^1\text{HNMR}$  (DMSO- $d_6$ , ppm): 2.87 (m,  $J = 7.2$  Hz, 4H, 2( $\text{CH}_2$ )), 3.40 (s, 2H,  $\text{CH}_2$ ), 3.45 (t,  $J = 7.2$  Hz, 4H, 2( $\text{CH}_2$ )), 3.76 (s, 3H,

CH<sub>3</sub>), 6.49-6.91 (m, 4H, aromatic proton), 6.92-8.38 (m, 5H, quinazoline); **MS** (m/z) 377.20 (M<sup>+</sup>, 1.17).

#### 4.1.1.7 4-Chloro-2-[1-(quinazolin-4-yl-carbamoyl)-ethylamino]-benzoic acid (Va):

Yield 75%; m.p 120-121°C. Analysis for C<sub>18</sub>H<sub>15</sub>ClN<sub>4</sub>O<sub>3</sub> (m.w 370); calcd: C, 58.31, H, 4.08, N, 15.11, Found: C 58.87, H 4.07, N, 15.13. **IR (KBr, cm<sup>-1</sup>):** 3497-3220 (OH), 3373-3320 (2NH), 1720 (C=O acid), 1665 (C=O amide), <sup>1</sup>HNMR (DMSO-d<sub>6</sub>, ppm): 1.14 (d, *J* = 7.2, 3H, CH<sub>3</sub>), 3.03 (m, 1H, CH), 6.41-6.91 (m, 3H, aromatic proton), 7.40-8.29 (m, 5H, quinazoline), 8.37 (s, 1H, NH) (D<sub>2</sub>O exchange), 8.30 (s, 1H, 1NH) (D<sub>2</sub>O exchange), 8.70 (s, 1H, OH) (D<sub>2</sub>O exchangeable), **MS** (m/z) 370.95, (M<sup>+</sup>, 12.12%).

#### 4.1.1.8 2-Indol-1-yl-N-quinazolin-4-yl-propionamide (Vb):

Yield 75%; m.p 283-285°C. Analysis for C<sub>19</sub>H<sub>16</sub>N<sub>4</sub>O (m.w 316); calcd: C, 72.13, H, 5.10, N, 17.71, Found: C, 72.22, H, 4.99, N, 17.73. **IR (KBr, cm<sup>-1</sup>):** 3430 (NH), 1687 (C=O), <sup>1</sup>HNMR (DMSO-d<sub>6</sub>, ppm): 1.81 (d, *J* = 8.0, 3H, CH<sub>3</sub>), 3.30 (m, 1H, CH), 7.50-8.41 (m, 5H, quinazoline), 6.29-7.02 (m, 6H, indole), 10.90 (s, 1H, NH) (D<sub>2</sub>O exchangeable); **MS** (m/z) 316.05, (M<sup>+</sup>, 2.59%).

#### 4.1.1.9 2-(4-Phenyl-piperazin-1-yl)-N-quinazolin-4-yl-propionamide Vc:

Yield 75%; m.p 120-121°C. Analysis for C<sub>21</sub>H<sub>23</sub>N<sub>5</sub>O (m.w 361); calcd: C, 69.78, H, 6.41, N, 19.38, Found C, 69.50, H, 6.40, N, 19.21. **IR (KBr, cm<sup>-1</sup>):** 3383 (NH), 1682 (C=O), <sup>1</sup>HNMR (DMSO-d<sub>6</sub>, ppm): 1.11 (d, 3H, CH<sub>3</sub>), 2.50 (t, *J* = 6.2 Hz, 4H, 2(CH<sub>2</sub>)), 3.00 (t, *J* = 6.2 Hz, 4H, 2(CH<sub>2</sub>)), 3.67 (m, 1H, CH), 7.13-7.60 (m, 5H, aromatic proton), 7.56-8.41 (s, 5H, quinazoline); **MS** (m/z) 361.30, (M<sup>+</sup>, 4.18%).

#### 4.1.1.10 2-Morpholin-4-yl-N-quinazolin-4-yl-propionamide (Vd):

Yield 75%; m.p 212-213°C. Analysis for C<sub>15</sub>H<sub>18</sub>N<sub>4</sub>O<sub>2</sub> (m.w 286); calcd: C, 62.92, H, 6.34, N, 19.57, Found C, 62.94, H, 6.40, N, 19.60. **IR (KBr, cm<sup>-1</sup>):** 3423 (NH), 1664 (C=O), <sup>1</sup>HNMR (DMSO-d<sub>6</sub>, ppm): 1.14 (d, *J* = 7.4, 3H, CH<sub>3</sub>), 2.40 (t, *J* = 6.0 Hz, 4H, 2(CH<sub>2</sub>)), 3.70 (t, *J* = 6.0 Hz 4H, 2(CH<sub>2</sub>)), 3.74 (m, 1H, CH), 7.70-8.31 (m, 5H, quinazoline), 8.50 (s, 1H, NH), **MS** (m/z) 286.10 (M<sup>+</sup>, 0.03%).

#### 4.1.2 General procedure for the preparation of 1-substituted-3-quinazolin-4-yl-urea (VIa-d):

To a solution of compound I (1.90 g, 10.00 mmol) in dry benzene (30 mL) was added the appropriate isocyanate/ isothiocyanate derivatives (50.00 mmol) (*viz.*: *p*-chlorophenylisocyanate, *m*-chlorophenylisocyanate, chloro ethylisocyanate and chloro ethylisothiocyanate) and the mixture was stirred for 24 hrs. The precipitated solid was collected by filtration, washed with dry benzene and

recrystallized from ethanol to give the titled compounds VIa-d.

#### 4.1.2.1 1-(4-Chlorophenyl)-3-quinazolin-4-yl-urea (VIa):

Yield 87.3%; m.p 215-217°C. Analysis for C<sub>15</sub>H<sub>11</sub>ClN<sub>4</sub>O (m.w 298); calcd: C, 60.31, H, 3.71, N, 18.76, Found C, 60.61, H, 3.94, N, 18.50. **IR (KBr, cm<sup>-1</sup>):** 3238-3158 (2NH), 1691 (C=O) <sup>1</sup>HNMR (DMSO-d<sub>6</sub>, Ppm): 5.04 (s, 1H, NH) (D<sub>2</sub>O exchangeable), 6.91 (dd, *J* = 8.5, 3.5 Hz, 2H, *m*-CH), 7.19 (dd, *J* = 8.0, 3.5 Hz, 2H, *o*-CH), 7.81- 8.43 (m, 5H, quinazoline), 8.20 (s, 1H, NH) (D<sub>2</sub>O exchange), **MS** (m/z) 298.95, (M<sup>+</sup>, 0.60%).

#### 4.1.2.2 1-(3-Chlorophenyl)-3-quinazolin-4-yl-urea (VIb):

Yield 86.4%; m.p 210-211°C. Analysis for C<sub>15</sub>H<sub>11</sub>ClN<sub>4</sub>O (m.w 298); calcd: C, 60.31, H, 3.71, N, 18.76, Found C, 60.60, H, 3.60, N, 18.70. **IR (KBr, cm<sup>-1</sup>):** 3238-3245 (2NH), 1695 (C=O), <sup>1</sup>HNMR (DMSO-d<sub>6</sub>, ppm): 6.51-7.03 (m, 4H, aromatic proton) 7.72-8.38 (m, 5H, quinazoline), 8.96 (2s, 2H, 2NH) (D<sub>2</sub>O exchangeable), **MS** (m/z) 298.95, (M<sup>+</sup>, 4.19).

#### 4.1.2.3 1-(2-Chloroethyl)-3-quinazolin-4-yl-urea (VIc):

Yield 93.5%; m.p 180-182°C. Analysis for C<sub>11</sub>H<sub>11</sub>ClN<sub>4</sub>O (m.w 250); calcd: C, 52.70, H, 4.42, N, 22.35, Found C, 52.92, H, 4.54, N, 22.36. **IR (KBr, cm<sup>-1</sup>):** 3368-3145 (2NH), 1673 (C=O) <sup>1</sup>HNMR (DMSO-d<sub>6</sub>, ppm): 3.60 (t, *J* = 7.4 Hz, 2H, CH<sub>2</sub>), 3.90 (t, *J* = 6.0 Hz, 2H, CH<sub>2</sub>), 7.70-8.81 (m, 5H, quinazoline), 10.31 (s, 2H, 2NH) (D<sub>2</sub>O exchangeable), **MS** (m/z) 250.10, (M<sup>+</sup>, 2.59%).

#### 4.1.2.4 1-(2-Chloroethyl)-3-quinazolin-4-yl-thiourea (VI d):

yield 94.5%; m.p 238-240°C. Analysis for C<sub>11</sub>H<sub>11</sub>ClN<sub>4</sub>S (m.w 266.7); calcd: C, 49.53, H, 4.16, N, 21.00, Found C, 49.63, H, 4.69, N, 21.51. **IR (KBr, cm<sup>-1</sup>):** 3495-3389 (2NH), 1110 (C=S) <sup>1</sup>HNMR (DMSO-d<sub>6</sub>, ppm): 3.90 (t, *J* = 6.2 Hz, 2H, CH<sub>2</sub>), 4.21 (t, *J* = 6.0 Hz 2H, CH<sub>2</sub>), 7.70- 8.73 (m, 5H, quinazoline), 10.30 (s, 2H, 2NH) (D<sub>2</sub>O exchangeable), **MS** (m/z) 266.40, (M<sup>+</sup>, 10.28%).

#### 4.1.3 General procedure for the preparation of 1-(2-Substituted ethyl)-3-quinazolin-4-yl-urea (VIIa-b):

A solution of 1-(2-chloro-ethyl)-3-quinazolin-4-yl-urea VIc (0.50 g, 2.00 mmol) is added to amine derivatives (20.00 mmol) in absolute ethanol (15 mL) and anhydrous sodium carbonate (0.49 g, 5.00 mmol). The mixture was heated under reflux for 12 hrs. The excess ethanol was evaporated under vacuum; and the residue was treated with 5% sodium bicarbonate solution to remove acid impurities, filtered, washed with water and dried to afford the titled compound.

#### 4.1.3.1 1-(2-Morpholin-4-yl-ethyl)-3-quinazolin-4-yl-urea (VIIa):

Yield 70%; m.p 234-235°C. Analysis for C<sub>15</sub>H<sub>19</sub>N<sub>5</sub>O<sub>2</sub> (m.w 301.3); calcd: C, 59.79, H, 6.36, N, 23.24, Found C, 60.10, H, 6.40, N, 23.20. **IR (KBr, cm<sup>-1</sup>):** 3381-3279 (2NH), 1624 (C=O), <sup>1</sup>HNMR (DMSO-d<sub>6</sub>, ppm): 2.41 (t, *J* = 6.0 Hz, 2H, 2(CH<sub>2</sub>)), 3.60 (t, *J* = 6.2 Hz, 4H, 2(CH<sub>2</sub>)), 3.90 (t, *J* = 6.4 Hz, 2H, CH<sub>2</sub>), 4.03 (t, *J* = 6.0 Hz, 4H, 2(CH<sub>2</sub>)), 7.23 (s, 1H, NH, D<sub>2</sub>O exchangeable), 7.31- 8.81 (m, 5H, quinazoline), 9.90 (s, 1H, NH) (D<sub>2</sub>O exchangeable), **MS (m/z)** 301.30, (M<sup>+</sup>, 0.6%).

#### 4.1.3.2 1-[2(4-Phenyl-piperazin-1-yl)-ethyl]-3-quinazolin-4-yl-urea (VIIIb):

Yield 68%; m.p 270-272°C. Analysis for C<sub>21</sub>H<sub>24</sub>N<sub>6</sub>O (m.w 376.4); calcd: C, 66.94, H, 6.43, N, 22.32, Found C, 66.40, H, 6.40, N, 22.50. **IR (KBr, cm<sup>-1</sup>):** 3496-3385 (2NH), 1677 (C=O) <sup>1</sup>HNMR (DMSO-d<sub>6</sub>, ppm): 3.12 (t, *J* = 6.0 Hz, 2H, CH<sub>2</sub>), 3.30 (t, *J* = 6.0 Hz, 2H, CH<sub>2</sub>), 3.50 (t, *J* = 6.2 Hz, 4H, 2(CH<sub>2</sub>)), 3.70 (t, *J* = 6.0 Hz, 4H, 2(CH<sub>2</sub>)), 6.90 -7.31 (m, 5H, aromatic proton), 7.59-8.40 (m, 5H, quinazoline), **MS (m/z)** 376.20, (M<sup>+</sup> 3.99%).

### 4.2 Biological evaluation of compounds:

#### 4.2.1 In-Vitro anticancer evaluation:

Potential cytotoxicity of the compounds was tested using the method of Skehan *et al.* [24]. Cells were plated in 96-multiwell plate (104 cells/well) for 24 hrs before treatment with the compound to allow the attachment of cell to the wall of the plate. Different concentration of the compounds under test (0, 1, 2, 5 and 10 ug/ml) was added to the cell monolayer triplicate wells were prepared for each individual dose. Monolayer cells were incubated with the compound for 48 hrs at 37°C and in atmosphere of 5% CO<sub>2</sub>. After 48 hrs. Cells were fixed, washed and stained with Sulfo-Rhodamine-B stain. Excess stain was washed with acetic acid and attached stain was recovered with *tris*-EDTA buffer. Color intensity was measured in an ELISA reader. The relation between surviving fraction and drug concentration is plotted to get the survival curve of each tumor cell line after the specific compound.

#### 4.2.2 Enzyme inhibition assay:

The In-vitro enzyme inhibition determination for the synthesized compounds was carried out in KINEXUS Corporation, Vancouver, British Columbia, Canada. Kinexus uses a radioactive assay format for profiling evaluation of protein kinase targets and all assays are performed in a designated radioactive working area. Protein kinase assays were performed at 30°C for 20-40 minutes (depending on the target) in a final volume of 25 according to the following assay reaction receipt: 5 µL of diluted active protein kinase target (~10-50 nM final protein concentration in the assay), 5 µL of peptide substrate, 5 µL kinase assay buffer, 5 µL of compound (various concentrations) and 5 µL of 33P-ATP (250 uM stock

solution, 0.8 µl Ci). The assay was initiated by the addition of 33P-ATP and the reaction mixture incubated at 30°C for 20-40 minutes, depending on the protein kinase target. After the incubation period, the assay was terminated by spotting 10 µl of the reaction mixture into multiscreen phosphocellulose P81 plate. The Multiscreen phosphocellulose P81 plate was washed 3 times for approximately 15 minutes each in a 1% phosphoric acid solution. The radioactivity on the P81 plate was counted in the presence of scintillation fluid in a Trilux scintillation counter. Blank control was set up for each protein kinase target which included all the assay components except the addition of appropriate substrate (replace with equal volume of kinase assay buffer). The corrected activity for PI3K target was determined by removing the blank control value [38, 39].

### 4.3. Molecular modeling:

Molecular docking study was conducted first using Glide software predicting the binding modes and affinities of compounds when they interact with protein binding site, then further explanation was conducted using C-Docker 2.5 software in the interface of Accelry's discovery studio 2.5 (Accelrys Inc., San Diego, CA, USA), in the computer drug design lab in pharmaceutical chemistry department, faculty of pharmacy, Ain Shams University.

#### 4.3.1 Protein preparation for docking using glide program:

Crystal structure of VEGFR2 in complex with benzimidazole-urea inhibitor (PDB code 2OH4) [37], was retrieved from the Protein Data Bank. The downloaded structure was prepared using the standard protocol in the Protein Preparation Wizard in Maestro (version 9.2, Schrödinger, LLC, New York, NY, 2011). Hydrogens were added, bond orders for proteins and ligand were corrected and partial charges were calculated from the OPLS\_2005 forcefield [40]. Protonation states were assigned by Epik [41]. Orientations of added hydrogens were extensively sampled for optimal H-bond formation and the model was then refined by minimization within heavy-atom RMSD of 0.3 Å to the crystal structure configuration. Eventually, the fully-atomistic ligand-protein complex was used in the subsequent modeling steps.

#### 4.3.2 Protein preparation for docking using Accelry's discovery studio 2.5.

##### Program:

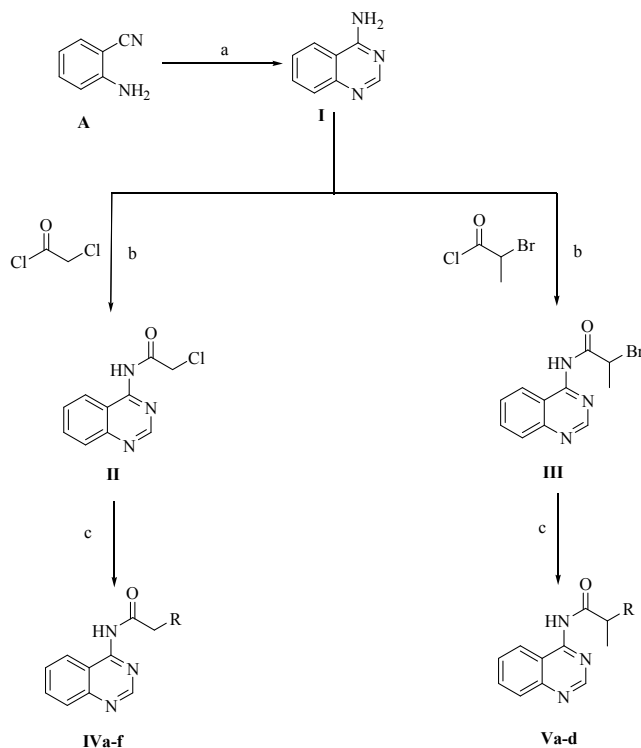
The coordinates of the kinase structure VEGFR-2 was obtained from the Protein Data Bank at the Research Collaboration for Structural Bioinformatics (RCSB) website [[www.rcsb.org](http://www.rcsb.org)]. PDB ID is 2OH4. The protein structure was prepared according to the standard protein preparation procedure integrated in Accelry's discovery studio 2.5. This was accomplished by adding hydrogen atoms, completing



the missing loops and applying force field parameters by using CHARMM force field [42]. All the water molecules in the protein were deleted. The protein

structure was minimized using steepest descent minimization algorithm. The ligand structure was removed from the binding sites.

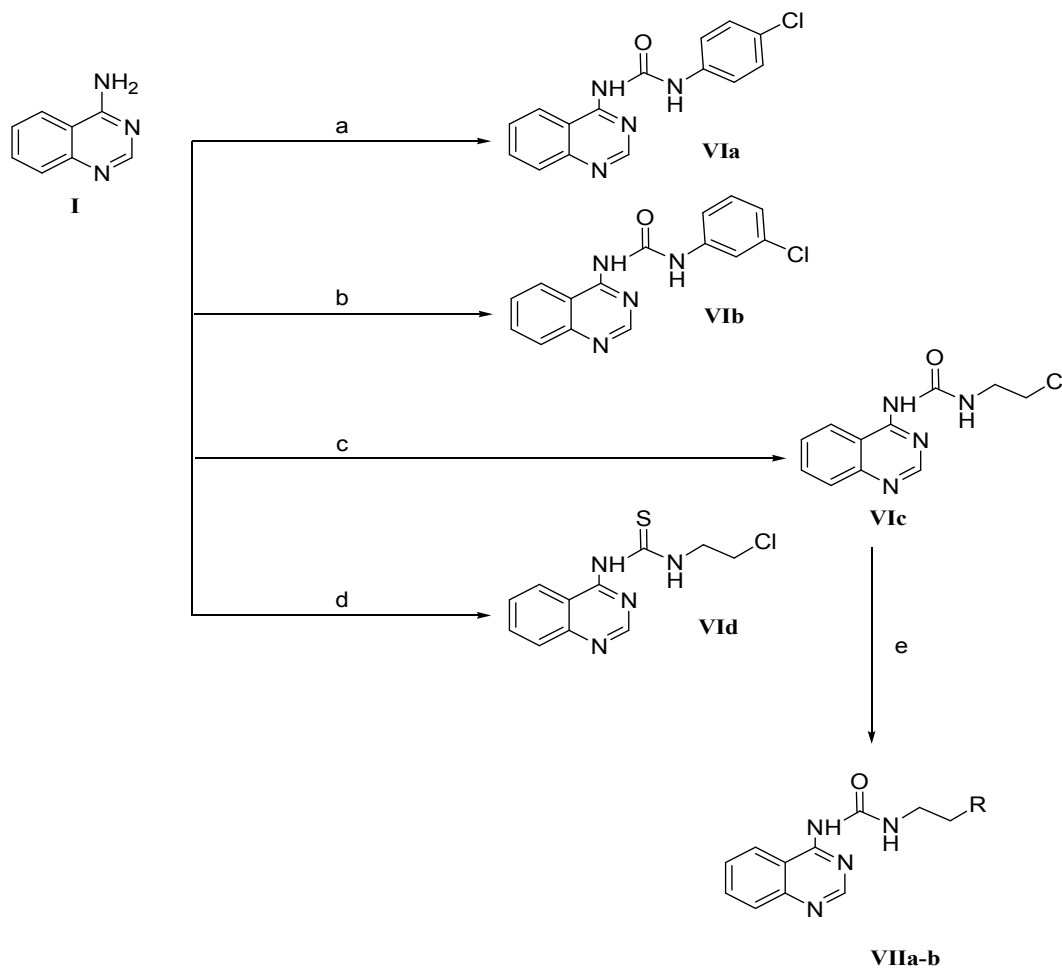
**Scheme 1: Synthesis of target compounds IVa-f and Va-d.**



	<b>R</b>		<b>R</b>
<b>a</b>		<b>d</b>	
<b>b</b>		<b>e</b>	
<b>c</b>		<b>f</b>	

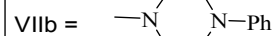
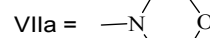
Reagents and conditions:  
 (a) Formamide, reflux, 2h  
 (b) Dry benzene/TEA, reflux, 9-10h  
 (c) Amines/abs. ethanol/TEA, reflux, 8-12h

**Scheme 2: Synthesis of target compounds VIa-d and VIIa,b:**



## Reagents and conditions;

- (a) p-Chlorophenylisocyanate/drybenzene, reflux, 24h  
 (b) m-Chlorophenylisocyanate/dry benzene, reflux, 24h  
 (c) Chloroethylisocyanate/dry benzene, reflux, 24h  
 (d) Chloroethylisothiocyanate/drybenzene, reflux, 24h  
 (e) Morpholine or Phenylpiperazine /abs. ethanol/anhydrous sodium carbonate

**Correspondence Author:**

Wgdan.Metwally,  
 Pharmaceutical chemistry Department, Faculty of  
 Pharmacy, Modern Science and Arts  
 University.Egypt.  
 Email: [wgdan\\_metwally@hotmail.com](mailto:wgdan_metwally@hotmail.com)

**References**

- Schnur, R.C., A.F. Fliri, S. Kajiji, and V.A. Pollack, N-(5-fluorobenzothiazol-2-yl)-2-guanidinothiazole-4-carboxamide. A novel, systemically active antitumor agent effective against 3LL Lewis lung carcinoma. *J Med Chem* 1991,34; 914-8.
- Hicklin, D.J. and L.M. Ellis, Role of the vascular endothelial growth factor pathway in tumor growth and angiogenesis. *J Clin Oncol* 2005,23; 1011-27.
- Ferrara, N., Vascular endothelial growth factor: basic science and clinical progress. *Endocr Rev* 2004,25; 581-611.
- Ferrara, N., H.P. Gerber, and J. LeCouter, The biology of VEGF and its receptors. *Nat Med* 2003,9; 669-76.
- Traxler, P., Tyrosine kinases as targets in cancer therapy - successes and failures. *Expert Opin Ther Targets* 2003,7; 215-34.
- Boehm, T., J. Folkman, T. Browder, and M.S. O'Reilly, Antiangiogenic therapy of experimental

- cancer does not induce acquired drug resistance. *Nature* 1997,390; 404-7.
7. Holmes, K., O.L. Roberts, A.M. Thomas, and M.J. Cross, Vascular endothelial growth factor receptor-2: structure, function, intracellular signalling and therapeutic inhibition. *Cell Signal* 2007,19; 2003-12.
  8. Jain, R.K., D.G. Duda, J.W. Clark, and J.S. Loeffler, Lessons from phase III clinical trials on anti-VEGF therapy for cancer. *Nat Clin Pract Oncol* 2006,3; 24-40.
  9. Gupta, K. and J. Zhang, Angiogenesis: a curse or cure? *Postgrad Med J* 2005,81; 236-42.
  10. Jain, R.K., Normalization of tumor vasculature: an emerging concept in antiangiogenic therapy. *Science* 2005,307; 58-62.
  11. de Vries, C., J.A. Escobedo, H. Ueno, K. Houck, N. Ferrara, and L.T. Williams, The fms-like tyrosine kinase, a receptor for vascular endothelial growth factor. *Science* 1992,255; 989-91.
  12. Shalaby, F., J. Rossant, T.P. Yamaguchi, M. Gertsenstein, X.F. Wu, M.L. Breitman, and A.C. Schuh, Failure of blood-island formation and vasculogenesis in Flk-1-deficient mice. *Nature* 1995,376; 62-6.
  13. Yang, J.C., L. Haworth, R.M. Sherry, P. Hwu, D.J. Schwartzentruber, S.L. Topalian, S.M. Steinberg, H.X. Chen, and S.A. Rosenberg, A randomized trial of bevacizumab, an anti-vascular endothelial growth factor antibody, for metastatic renal cancer. *N Engl J Med* 2003,349; 427-34.
  14. Mendel, D.B., A.D. Laird, X. Xin, S.G. Louie, J.G. Christensen, G. Li, R.E. Schreck, T.J. Abrams, T.J. Ngai, L.B. Lee, L.J. Murray, J. Carver, E. Chan, K.G. Moss, J.O. Haznedar, J. Sukbuntherng, R.A. Blake, L. Sun, C. Tang, T. Miller, S. Shirazian, G. McMahon, and J.M. Cherrington, In vivo antitumor activity of SU11248, a novel tyrosine kinase inhibitor targeting vascular endothelial growth factor and platelet-derived growth factor receptors: determination of a pharmacokinetic/pharmacodynamic relationship. *Clin Cancer Res* 2003,9; 327-37.
  15. Hess-Stumpp, H., M. Haberey, and K.H. Thierauch, PTK 787/ZK 222584, a tyrosine kinase inhibitor of all known VEGF receptors, represses tumor growth with high efficacy. *Chembiochem* 2005,6; 550-7.
  16. Wedge, S.R., D.J. Ogilvie, M. Dukes, J. Kendrew, R. Chester, J.A. Jackson, S.J. Boffey, P.J. Valentine, J.O. Curwen, H.L. Musgrove, G.A. Graham, G.D. Hughes, A.P. Thomas, E.S. Stokes, B. Curry, G.H. Richmond, P.F. Wadsworth, A.L. Bigley, and L.F. Hennequin, ZD6474 inhibits vascular endothelial growth factor signaling, angiogenesis, and tumor growth following oral administration. *Cancer Res* 2002,62; 4645-5655.
  17. Batchelor, T.T., A.G. Sorensen, E. di Tomaso, W.T. Zhang, D.G. Duda, K.S. Cohen, K.R. Kozak, D.P. Cahill, P.J. Chen, M. Zhu, M. Ancukiewicz, M.M. Mrugala, S. Plotkin, J. Drappatz, D.N. Louis, P. Ivy, D.T. Scadden, T. Benner, J.S. Loeffler, P.Y. Wen, and R.K. Jain, AZD2171, a pan-VEGF receptor tyrosine kinase inhibitor, normalizes tumor vasculature and alleviates edema in glioblastoma patients. *Cancer Cell* 2007,11; 83-95.
  18. Wedge, S.R., J. Kendrew, L.F. Hennequin, P.J. Valentine, S.T. Barry, S.R. Brave, N.R. Smith, N.H. James, M. Dukes, J.O. Curwen, R. Chester, J.A. Jackson, S.J. Boffey, L.L. Kilburn, S. Barnett, G.H. Richmond, P.F. Wadsworth, M. Walker, A.L. Bigley, S.T. Taylor, L. Cooper, S. Beck, J.M. Jurgensmeier, and D.J. Ogilvie, AZD2171: a highly potent, orally bioavailable, vascular endothelial growth factor receptor-2 tyrosine kinase inhibitor for the treatment of cancer. *Cancer Res* 2005,65; 4389-400.
  19. Goffin, J.R., I.C. Anderson, J.G. Supko, J.P. Eder, Jr., G.I. Shapiro, T.J. Lynch, M. Shipp, B.E. Johnson, and A.T. Skarin, Phase I trial of the matrix metalloproteinase inhibitor marimastat combined with carboplatin and paclitaxel in patients with advanced non-small cell lung cancer. *Clin Cancer Res* 2005,11; 3417-24.
  20. Whittles, C.E., T.M. Pocock, S.R. Wedge, J. Kendrew, L.F. Hennequin, S.J. Harper, and D.O. Bates, ZM323881, a novel inhibitor of vascular endothelial growth factor-receptor-2 tyrosine kinase activity. *Microcirculation* 2002,9; 513-22.
  21. Hennequin, L.F., Crawley, G. Charles, L.F. Andre, McKerrecher, J. Philip, and Lambert, *Preparation of quinazolinyureas and analogs as VEGF receptor antagonists*. 2001, AstraZeneca AB, Swed.; AstraZeneca UK Limited.
  22. Kroe, R.R., J. Regan, A. Proto, G.W. Peet, T. Roy, L.D. Landro, N.G. Fuschetto, C.A. Pargellis, and R.H. Ingraham, Thermal denaturation: a method to rank slow binding, high-affinity P38alpha MAP kinase inhibitors. *J Med Chem* 2003,46; 4669-75.
  23. Gago, F., Stacking interactions and intercalative DNA binding. *Methods* 1998,14; 277-92.
  24. Skehan, P., R. Storeng, D. Scudiero, A. Monks, J. McMahon, D. Vistica, J.T. Warren, H. Bokesch, S. Kenney, and M.R. Boyd, New colorimetric cytotoxicity assay for anticancer-

- drug screening. *J Natl Cancer Inst* 1990,82; 1107-12.
25. Tsou, H.R., N. Mamuya, B.D. Johnson, M.F. Reich, B.C. Gruber, F. Ye, R. Nilakantan, R. Shen, C. Discafani, R. DeBlanc, R. Davis, F.E. Koehn, L.M. Greenberger, Y.F. Wang, and A. Wissner, 6-Substituted-4-(3-bromophenylamino)quinazolines as putative irreversible inhibitors of the epidermal growth factor receptor (EGFR) and human epidermal growth factor receptor (HER-2) tyrosine kinases with enhanced antitumor activity. *J Med Chem* 2001,44; 2719-34.
  26. Jones, G., P. Willett, R.C. Glen, A.R. Leach, and R. Taylor, Development and validation of a genetic algorithm for flexible docking. *J Mol Biol* 1997,267; 727-48.
  27. Ewing, T.J., S. Makino, A.G. Skillman, and I.D. Kuntz, DOCK 4.0: search strategies for automated molecular docking of flexible molecule databases. *J Comput Aided Mol Des* 2001,15; 411-28.
  28. Abagyan, R. and M. Totrov, High-throughput docking for lead generation. *Curr Opin Chem Biol* 2001,5; 375-82.
  29. Welch, W., J. Ruppert, and A.N. Jain, Hammerhead: fast, fully automated docking of flexible ligands to protein binding sites. *Chem Biol* 1996,3; 449-62.
  30. McMartin, C. and R.S. Bohacek, QXP: powerful, rapid computer algorithms for structure-based drug design. *J Comput Aided Mol Des* 1997,11; 333-44.
  31. Murray, C.W., C.A. Baxter, and A.D. Frenkel, The sensitivity of the results of molecular docking to induced fit effects: application to thrombin, thermolysin and neuraminidase. *J Comput Aided Mol Des* 1999,13; 547-62.
  32. McGann, M.R., H.R. Almond, A. Nicholls, J.A. Grant, and F.K. Brown, Gaussian docking functions. *Biopolymers* 2003,68; 76-90.
  33. Rarey, M., B. Kramer, T. Lengauer, and G.A.A. Klebe, fast flexible docking method using an incremental construction algorithm. *Chem. Biol.* 1996,261; 470-89.
  34. Charifson, P.S., J.J. Corkery, M.A. Murcko, and W.P. Walters, Consensus scoring: A method for obtaining improved hit rates from docking databases of three-dimensional structures into proteins. *J Med Chem* 1999,42; 5100-9.
  35. Bissantz, C., G. Folkers, and D. Rognan, Protein-based virtual screening of chemical databases. 1. Evaluation of different docking/scoring combinations. *J Med Chem* 2000,43; 4759-67.
  36. Stahl, M. and M. Rarey, Detailed analysis of scoring functions for virtual screening. *J Med Chem* 2001,44; 1035-42.
  37. Hasegawa, M., N. Nishigaki, Y. Washio, K. Kano, P.A. Harris, H. Sato, I. Mori, R.I. West, M. Shibahara, H. Toyoda, L. Wang, R.T. Nolte, J.M. Veal, and M. Cheung, Discovery of novel benzimidazoles as potent inhibitors of TIE-2 and VEGFR-2 tyrosine kinase receptors. *J Med Chem* 2007,50; 4453-70.
  38. Zahra Abdellah, Alireza Ahmadi, Shahana Ahmed, Matthew Aimable, Rachael Ainscough, Jeff Almeida, and Claire Almond, Finishing the euchromatic sequence of the human genome. *Nature* 2004,431; 931-45.
  39. Adrian, F.J., Q. Ding, T. Sim, A. Velentza, C. Sloan, Y. Liu, G. Zhang, W. Hur, S. Ding, P. Manley, J. Mestan, D. Fabbro, and N.S. Gray, Allosteric inhibitors of Bcr-abl-dependent cell proliferation. *Nat Chem Biol* 2006,2; 95-102.
  40. Kony, D., W. Damm, S. Stoll, and W.F. Van Gunsteren, An improved OPLS-AA force field for carbohydrates. *J Comput Chem* 2002,23; 1416-29.
  41. Shelley, J.C., A. Cholleti, L.L. Frye, J.R. Greenwood, M.R. Timlin, and M. Uchimaya, Epik: a software program for pKa prediction and protonation state generation for drug-like molecules. *J. Comput.-Aided Mol. Des.* 2007,21; 681-91.
  42. Brooks, B.R., CHARMM: A program for macromolecular energy, minimization, and dynamics calculations. *J Comput Chem* 4 1983; 187-217.